

Olga Dąbrowska  orcid.org/0000-0003-2594-5599

olga.dabrowska@pk.edu.pl

Cracow University of Technology, Institute of Structural Mechanics

Henryk Ciurej  orcid.org/0000-0003-4017-6185

hciurej@agh.edu.pl

AGH University of Science and Technology, Faculty of Mining and Geoen지니어ing

SENSITIVITY ANALYSIS OF THE DYNAMIC RESPONSE OF A FRAME.

PART II: HARMONIC AND SEISMIC EXCITATIONS

ANALIZA WRAŻLIWOŚCI ODPOWIEDZI DYNAMICZNEJ RAMY.

CZĘŚĆ II: WYMUSZENIE HARMONICZNE ORAZ SEJSMICZNE

Abstract

This paper is a continuation of the first part [7] where basic relations and derivatives related to the sensitivity analysis of the standard 3D beam element have been derived. This part presents the sensitivity analysis of dynamic response of a flat frame using the Direct Differentiation Method for harmonic and seismic excitations separately. Harmonic excitations are typically found if some equipment is placed on the stories of industrial buildings. In that case the practical benefit of determining the structure response and its derivatives allows to determine, for example, the vibration comfort of staff and determine the impact of particular structural parameters on the level of comfort. With regard to seismic excitations, determining the response of a structure and its derivatives allows to determine the level of impact of individual parameters on the response.

Keywords: sensitivity analysis, direct differentiation method, explicit differentiation

Streszczenie

Niniejszy tekst jest kontynuacją części pierwszej [7], w której wyprowadzono podstawowe relacje i pochodne związane z analizą wrażliwości standardowego elementu belkowego 3D. W niniejszym artykule przedstawiono analizę wrażliwości odpowiedzi dynamicznej ramy płaskiej metodą bezpośrednią przy wymuszeniach osobno harmonicznym oraz sejsmicznym. Rozważane zadanie jest liniowe. Wymuszenia harmoniczne są typowe przy lokalizacji rozmaitych urządzeń na stropach budynków przemysłowych. Praktyczna strona wyznaczenia odpowiedzi konstrukcji i jej pochodnych w takich sytuacjach pozwala określić np. komfort wibracyjny osób znajdujących się na konstrukcji oraz określić wpływ poszczególnych parametrów konstrukcyjnych na poziom tego komfortu. W odniesieniu do wymuszeń sejsmicznych wyznaczenie odpowiedzi konstrukcji oraz jej pochodnych pozwala rozstrzygnąć skalę wpływu poszczególnych parametrów na odpowiedź.

Słowa kluczowe: analiza wrażliwości, bezpośrednia analiza wrażliwości, pochodne równania ruchu

1. Introduction

This paper is a continuation of the first part [7], where basic relations and derivatives related to the sensitivity analysis of the standard 3D beam element have been derived.

Sensitivity analysis consists in searching for changes in physical quantities in relation to changes in selected parameters, which are called design variables, decision variables or free variables. Ultimately, the sensitivity analysis comes down to calculating derivatives of specific functions with respect to parameters [9]. These parameters can determine the configuration of the structure (i.e. its geometry), properties of materials, dimensions or characteristics of cross-sections, etc. If the parameters describe the geometry of the structure, then the sensitivity analysis is related to the determination of material derivatives [10].

This part presents the sensitivity analysis of dynamic response of a flat frame using the Direct Differentiation Method [10] separately for harmonic and seismic excitations. The presented problem is referenced in broad literature (see [1, 11, 8, 5, 6]).

Harmonic excitations are typically found if some equipment are placed on the binders of industrial buildings. In that case the practical benefit of determining the structure response and its derivatives that it allows to determine, for example, the vibration comfort of staff and determine the impact of particular structural parameters on the level of comfort.

With respect to seismic (kinematic) excitations, the equations of motion are expressed in relative displacements, that fact simplifies the right hand side of equation. Determination of structural response and its derivatives for seismic excitation allows to determine how individual parameters influence on the magnitude of the response.

In both cases, optimization problem should be formulated and solved. Solution with gradient method requires providing derivatives with respect to design parameters. Sensitivity analysis make it possible to obtain these derivatives

2. The subject of the analysis

Subject frame is shown in the Fig. 1. It is a three-nave flat reinforced concrete frame with perpendicular joints. The figure also depicted parametrisation of the geometry. The material parameters (for concrete) are: elastic modulus $E = 32$ GPa, density $\rho = 2500$ kg/m³. The common width of all bar sections is $b = 0.3$ m.

The vector of design parameters has the form:

$$\mathbf{h} = [l_1, l_2, H, h_z, h_w, h_r], \quad \mathbf{h} \in \mathcal{R}_+^{N_p}, \quad N_p = 6, \quad (1)$$

where: l_1 is the width of the left outer and inner naves, l_2 the width of the right nave, H is the height of the stories, h_z is the cross-sections height of the external pillars, h_w is the cross-section height of the inner pillars. The point in the design space \mathcal{R}_+^6 for which calculations will be made of both the dynamic frame responses and their derivatives is equal to $h_0 = [6.0, 6.0, 3.0, 0.4, 0.4, 0.6]$ m.

Proportional structural dissipation was assumed (see [3]) i.e.

$$\mathbf{C}(\mathbf{h}) = \alpha \mathbf{M}(\mathbf{h}) + \beta \mathbf{K}(\mathbf{h}), \quad (2)$$

where $\alpha = 0.02$, $\beta = 0.003$.

The Fig. 2 shows the division of the frame into finite elements. The pillars were divided into 12 elements, and the binders were divided into 24 elements. Each element has a length of 0.25 m. The lowest nodes are fixed. In this figure, the global coordinate system is marked also.

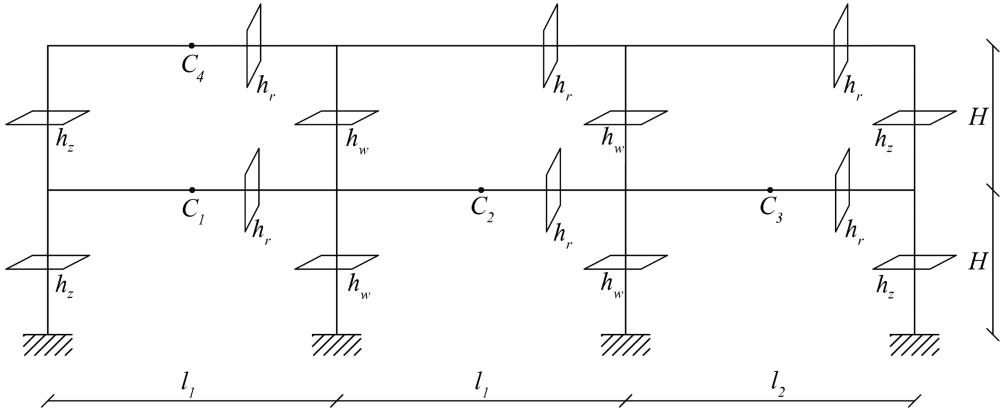


Fig. 1. Flat subject frame. Design parameters are shown. Points C_1, C_2, C_3 represent mean span of first level binders, point C_4 is the mean span of the upper binder of the left nave

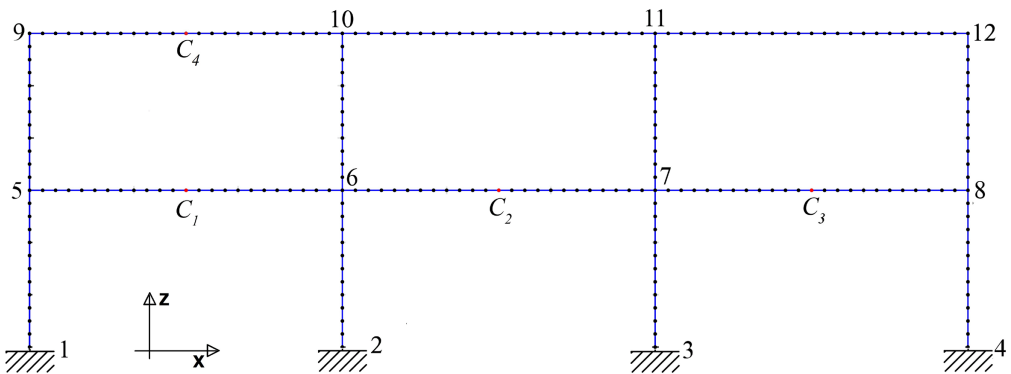


Fig. 2. Boundary conditions and numbering of nodes in the connections of girders and columns

The following Figs. 3, 4, 5 show three of the smallest eigenfrequencies $f_1 = 7.74$ Hz, $f_2 = 22.7$ Hz, $f_3 = 31.6$ Hz. The first two eigenmodes are related to the horizontal movement of binders (pillar bending), and the third eigenmode express vertical vibrations of the binders. The vertical and horizontal rulers allow to see the proportions of the eigenmodes.

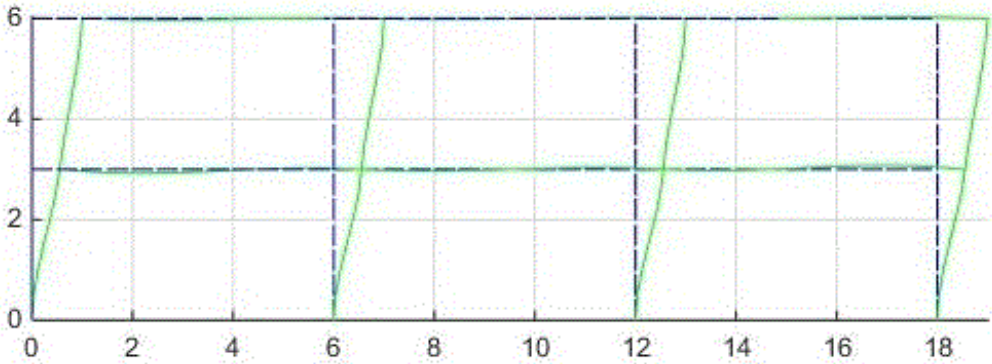


Fig. 3. First eigenmode of the frame $f_1 = 7.74$ Hz

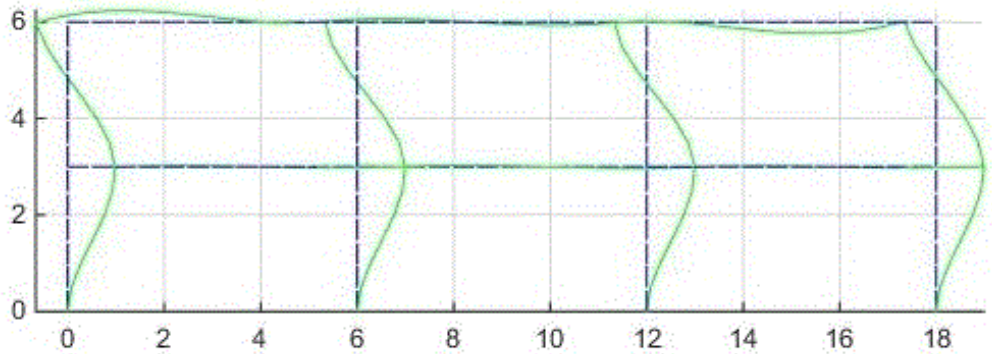


Fig. 4. Second eigenmode of the frame $f_2 = 22.7$ Hz

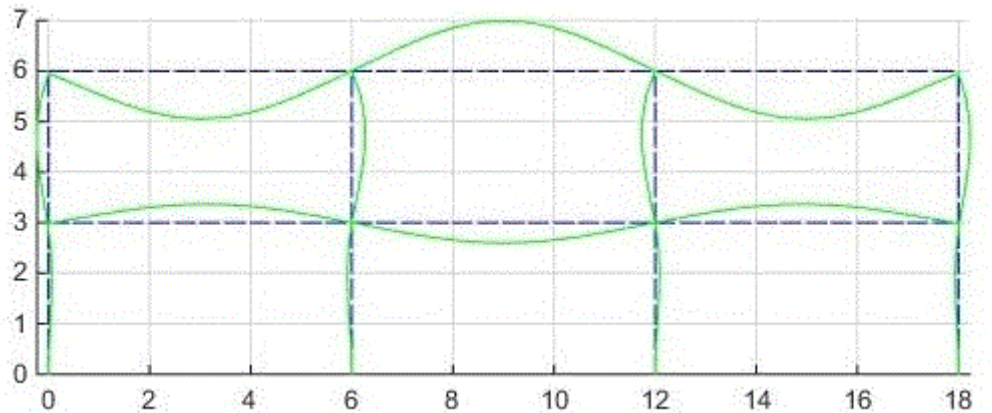


Fig. 5. Third eigenmode of the frame $f_3 = 31.6$ Hz

The aim of the paper is to determine displacements, velocities and accelerations as a function of time at the points: C_1 , C_2 , C_3 and C_4 and derivative of these quantities in relation to the design parameters (1) with two mutually exclusive types of vibration excitation:

1. The periodic excitations located in the points C_1 and C_2 – Fig. 6. The point C_1 is loaded with force $P_1(t) = P_{01} \sin(\omega_1 t)$, while point C_2 is loaded with force $P_2(t) = P_{02} \sin(\omega_2 t)$, where $P_{01} = 50$ kN, $\omega_1 = 37.5$ rad/s ($f_1 \approx 5.97$ Hz), $P_{02} = 65$ kN, $\omega_2 = 48.5$ rad/s ($f_2 \approx 7.72$ Hz). It means that response of the whole excitation and response of the frame are pseudoperiodic functions.

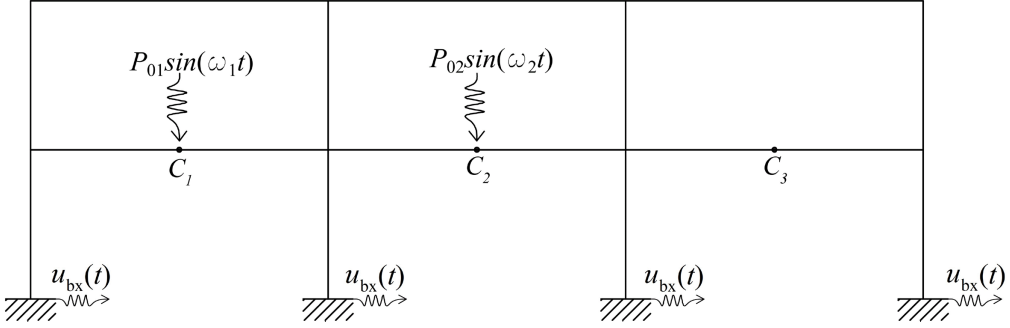


Fig. 6. Localization of excitations of: vertical harmonics P_1 i P_2 and horizontal seismic $u_{bx}(t)$

2. The horizontal seismic excitation $\ddot{u}_x(t)$ (Fig. 6) registered in El Centro in 1940. The diagram of ground accelerations is shown in Fig. 7. The diagram is taken from [4]. A broad discussion of this earthquake can be found in [12].

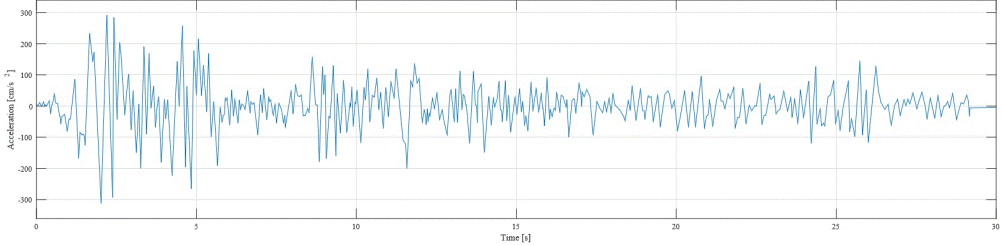


Fig. 7. Recorded diagram of horizontal ground accelerations $\ddot{u}_{bx}(t)$ in El Centro in 1940 [4]

3. Case no 1: harmonic excitation

The first example concern the harmonic excitation caused by two forces $P_1(t)$, $P_2(t)$ which are independent of the design parameters \mathbf{h} . These forces were applied in the middle of the binders at points C_1 and C_2 respectively. In the beginning the equation of motion (3) (see [7]) should be solved:

$$\mathbf{M}_{ss}(\mathbf{h})\ddot{\mathbf{x}}_s(\mathbf{h}) + \mathbf{C}_{ss}(\mathbf{h})\dot{\mathbf{x}}_s(\mathbf{h}) + \mathbf{K}_{ss}(\mathbf{h})\mathbf{x}_s(\mathbf{h}) = \mathbf{P}_{s1} \sin(\omega_1 t) + \mathbf{P}_{s2} \sin(\omega_2 t), \quad (3)$$

where the dependencies of vectors and matrices on the parameters \mathbf{h} are explicitly marked and the loads do not depend on the parameter vector. In matrices with indices $_{ss}$ the boundary

conditions were taken into account; vector \mathbf{x}_s means displacements of nodes unrestrained by the boundary conditions.

According to the DDM procedure the equation (3) should be directly differentiated with (2) taking into account:

$$\mathbf{M}_{ss} \frac{D\ddot{\mathbf{x}}_s}{Dh_p} + \mathbf{C}_{ss} \frac{D\dot{\mathbf{x}}_s}{Dh_p} + \mathbf{K}_{ss} \frac{D\mathbf{x}_s}{Dh_p} = - \left[\frac{D\mathbf{M}_{ss}}{Dh_p} (\ddot{\mathbf{x}}_s + \alpha \dot{\mathbf{x}}_s) + \frac{D\mathbf{K}_{ss}}{Dh_p} (\beta \dot{\mathbf{x}}_s + \mathbf{x}_s) \right], \quad p=1, \dots, N_p. \quad (4)$$

The following algorithm is result of both presented equations:

1. For a given vector of parameters \mathbf{h}_0 the equation (3) should be solved once.
2. For each parameter $h_p, p = 1, \dots, N_p$ (loop over index p):
 - (a) Find the material derivatives $D\mathbf{M}_{ss}/Dh_p$ and $D\mathbf{K}_{ss}/Dh_p$ in the equation (4).
 - (b) Using the solution from point 1 (i.e. $\ddot{\mathbf{x}}_s, \dot{\mathbf{x}}_s, \mathbf{x}_s$) aggregate the right hand side vector of the equation (4).
 - (c) Solve the equation (4).
3. Stop.

Due to the mathematical similarity of the equations (3) and (4) the same algorithm of time integration is used. In the present work the Newmark procedure [2] with the integration step $\Delta t = 0.001$ sec. is used. The loop in point 2 can be easily parallelized which would radically speed up the calculations.

The vertical displacements and accelerations and their derivatives at points C_1, C_2, C_3 are shown in the following Fig. 8 to Fig. 13. The time interval cover 2.0 sec. i.e. from 1.0 sec. up to 3.0 sec. As you can see after 1.0 sec. observed vibrations and derivatives functions with respect to all parameters are already steady-state.

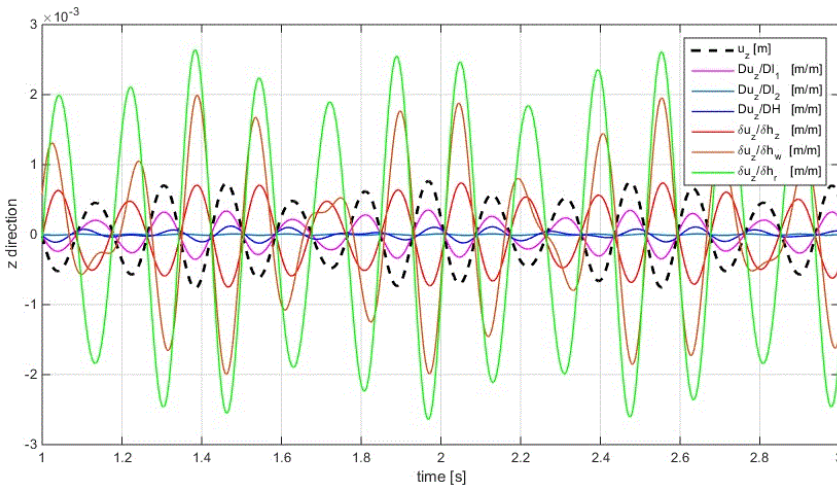


Fig. 8. Vertical displacement $u_z(t)$ at C_1 and derivative Du_z/Dh_p

To facilitate the interpretation of the obtained results, let introduce following designation:

$$g_{,h_p}^{\max} = \max_{t \in [1,3]} \left| \frac{\mathcal{D}g}{\mathcal{D}h_p} \right|, \quad (5)$$

which expresses the maximum absolute value of the derivative of $g(t, \mathbf{h})$ with respect to p -th parameter, the maximum being calculated over the time interval $t \in [1, 3]$ sec. i.e. in the time of steady-state vibrations

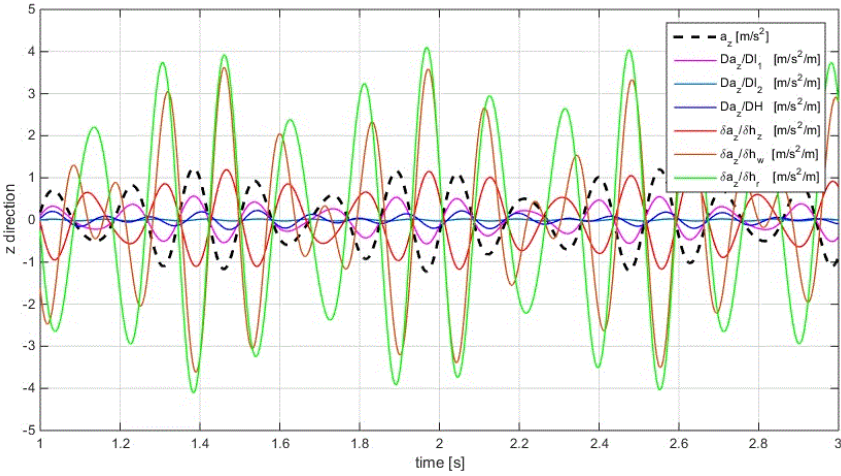


Fig. 9. Vertical acceleration $a_z(t)$ at C_1 and derivative $\mathcal{D}a_z/\mathcal{D}h_p$

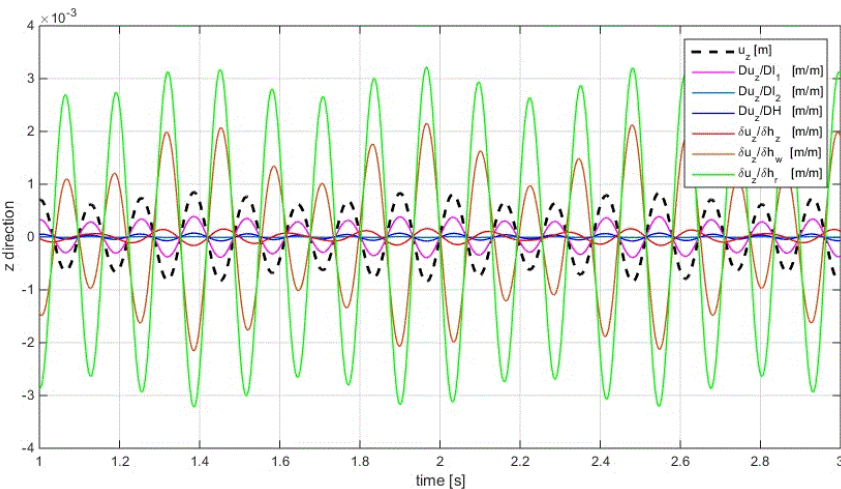


Fig. 10. Vertical displacement $u_z(t)$ at C_2 and derivative $\mathcal{D}u_z/\mathcal{D}h_p$

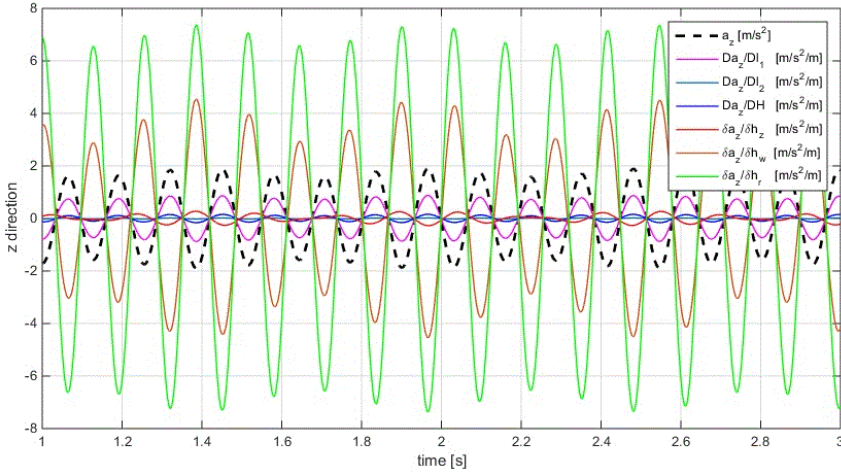


Fig. 11. Vertical acceleration $a_z(t)$ at C_2 and derivative $\mathcal{D}a_z/\mathcal{D}h_p$

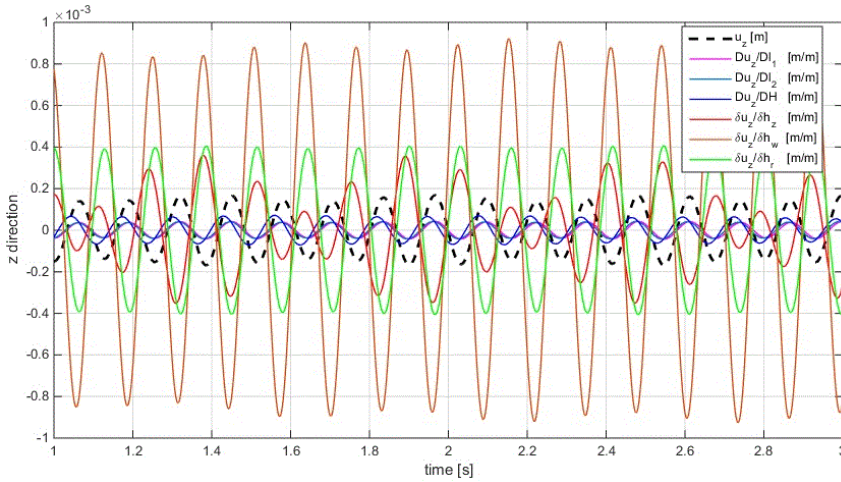


Fig. 12. Vertical displacement $u_z(t)$ at C_3 and derivative $\mathcal{D}u_z/\mathcal{D}h_p$

Observation of the results from the Fig. 8 to Fig. 13 allows to formulate the following conclusions:

1. At the point C_1 the parameters of h_r (cross-section height of the binders), h_w (cross-section height of the internal pillars) and h_z (cross-section height of the external pillars) have the greatest influence on the displacements and accelerations waveforms. Because there is $u_{z,h_r}^{\max} > u_{z,h_w}^{\max} > u_{z,h_z}^{\max}$ and $a_{z,h_r}^{\max} > a_{z,h_w}^{\max} > a_{z,h_z}^{\max}$. It should be emphasize that the derivatives remain in the counter-phase to the waveforms – thus increasing the stiffness of cross-sections will reduce the amplitudes of displacements and accelerations at point C_1 .

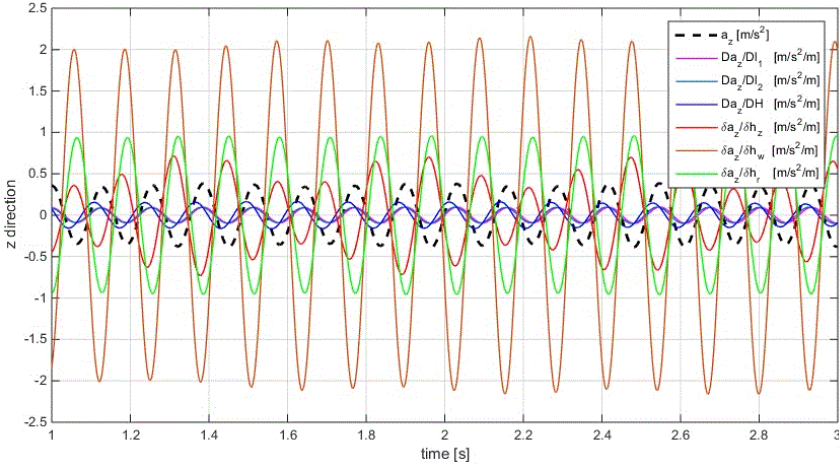


Fig. 13. Vertical acceleration $a_z(t)$ at C_3 and derivative $\mathcal{D}a_z/\mathcal{D}h_p$

2. At the point C_2 the parameters of h_r (cross-section height of the binders), h_w (cross-section height of the internal pillars) and l_1 (width of the naves) have the greatest influence on the displacements and accelerations waveforms. Because there is $u_{z,h_r}^{\max} > u_{z,h_w}^{\max} > u_{z,l_1}^{\max}$ and $a_{z,h_r}^{\max} > a_{z,h_w}^{\max} > a_{z,l_1}^{\max}$. It should be emphasize that the derivatives $\mathcal{D}/\mathcal{D}h_r$ and $\mathcal{D}/\mathcal{D}h_w$ remains in the counter-phase to the waveforms – thus increasing the stiffness of cross-sections will reduce the amplitudes of displacements and accelerations. In the opposition to the above is the derivative with regard to l_1 i.e. increase the length of the binders will cause an increase in the displacements or accelerations at the point C_2 .
3. At the point C_3 the parameters of h_w (cross-section height of the internal pillars), h_r (crosssection height of the binders) and h_z (cross-section height of the external pillars) have the greatest influence on the displacements and accelerations waveforms. Because there is $u_{z,h_w}^{\max} > u_{z,h_r}^{\max} > u_{z,h_z}^{\max}$ and $a_{z,h_w}^{\max} > a_{z,h_r}^{\max} > a_{z,h_z}^{\max}$. It should be emphasize that the derivatives remains in the counter-phase to the waveforms – thus increasing the stiffness of cross-sections will reduce the amplitudes of displacements and accelerations at the point C_3 .

4. Case no 2: seismic excitation

The second example concern the seismic excitation of the frame with horizontal ground accelerations recorded during the earthquake in El Centro [4].

The following is the state equation:

$$\begin{aligned} \mathbf{M}_{ss}(\mathbf{h})\ddot{\mathbf{y}}_s(\mathbf{h}) + \mathbf{C}_{ss}(\mathbf{h})\dot{\mathbf{y}}_s(\mathbf{h}) + \mathbf{K}_{ss}(\mathbf{h})\mathbf{y}_s(\mathbf{h}) &= \\ &= -[\mathbf{M}_{sb}(\mathbf{h}) - \mathbf{M}_{ss}(\mathbf{h})\mathbf{K}_{ss}^{-1}(\mathbf{h})\mathbf{K}_{sb}(\mathbf{h})]\mathbf{B}\ddot{\mathbf{u}}_b, \end{aligned} \quad (6)$$

where \mathbf{y} is the vector of relative displacement. Direct differentiation of (6) lead to relations:

$$\mathbf{M}_{ss} \frac{D\dot{\mathbf{y}}_s}{Dh_p} + \mathbf{C}_{ss} \frac{D\dot{\mathbf{y}}_s}{Dh_p} + \mathbf{K}_{ss} \frac{D\mathbf{y}_s}{Dh_p} = - \left[\frac{D\mathbf{M}_{ss}}{Dh_p} (\dot{\mathbf{y}}_s + \alpha \dot{\mathbf{y}}_s) + \frac{D\mathbf{K}_{ss}}{Dh_p} (\beta \dot{\mathbf{y}}_s + \mathbf{y}_s) \right] - \left[\frac{D\mathbf{M}_{sb}}{Dh_p} + \left(\mathbf{M}_{ss} \mathbf{K}_{ss}^{-1} \frac{D\mathbf{K}_{ss}}{Dh_p} - \frac{D\mathbf{M}_{ss}}{Dh_p} \right) \mathbf{K}_{ss}^{-1} \mathbf{K}_{sb} - \mathbf{M}_{ss} \mathbf{K}_{ss}^{-1} \frac{D\mathbf{K}_{sb}}{Dh_p} \right] \mathbf{B} \ddot{\mathbf{u}}_b, \quad p=1, \dots, N_p, \quad (7)$$

where the equation

$$\frac{D\mathbf{K}_{ss}^{-1}}{Dh_p} = -\mathbf{K}_{ss}^{-1} \frac{D\mathbf{K}_{ss}}{Dh_p} \mathbf{K}_{ss}^{-1}$$

is used. In the given dependencies, the matrix \mathbf{B} is a column of ones only in places corresponding to horizontal degrees of freedom fixed in the support nodes (in the considered problem the vector \mathbf{B} is not depend on \mathbf{h}) and the vector $\ddot{\mathbf{u}}_b$ turns under these circumstances into a scalar i.e. $\ddot{\mathbf{u}}_b(t) \equiv \ddot{u}_{bx}(t)$ and express the function of acceleration of horizontal soil vibrations.

Both of the presented equations lead to algorithm:

1. For a given vector of parameters \mathbf{h}_0 the equation (6) should be solved once.
2. Find matrix \mathbf{K}_{ss}^{-1} once.
3. For each parameter $h_p, p = 1, \dots, N_p$ (loop over index p):
 - (a) Find the material derivatives $D\mathbf{M}_{ss}/Dh_p$ and $D\mathbf{K}_{ss}/Dh_p$ in the equation (7).
 - (b) Using the solution from point 1 (i.e. $\dot{\mathbf{x}}_s, \dot{\mathbf{x}}_s, \mathbf{x}_s$) aggregate the right hand side vector of the equation (7).
 - (c) Solve equation (7).
4. Stop.

Like in previous example, the Newmark procedure [2] with the integration step $\Delta t = 0.001$ sec. is used. The loop in point 3 was parallelized and that fact radically speed up the calculations.

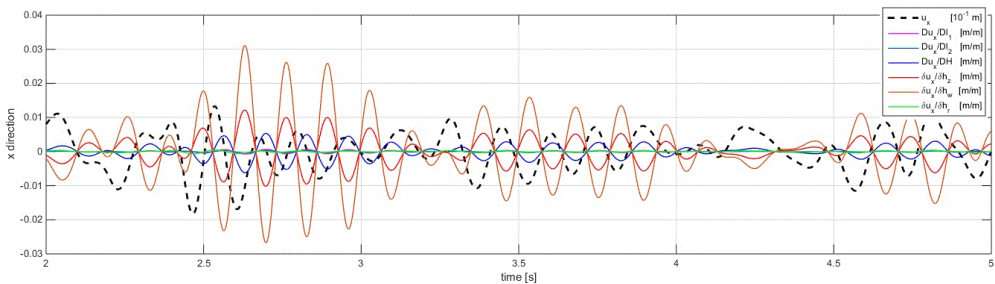


Fig. 14. Diagram of horizontal displacement $u_x(t)$ at C_1 and derivative Du_x/Dh_p

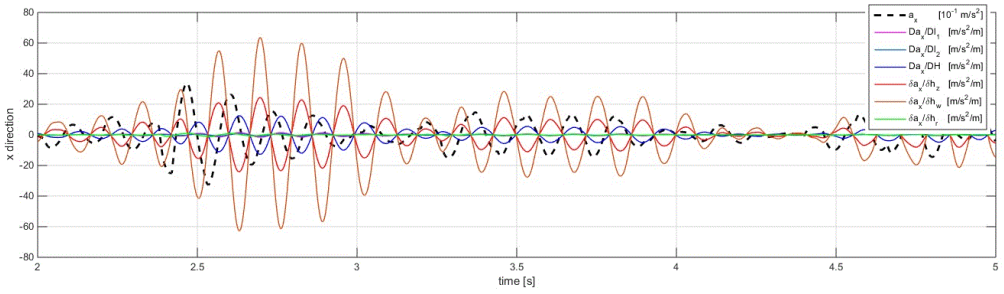


Fig. 15. Diagram of horizontal acceleration $a_x(t)$ at C_1 and derivative Da_x/Dh_p

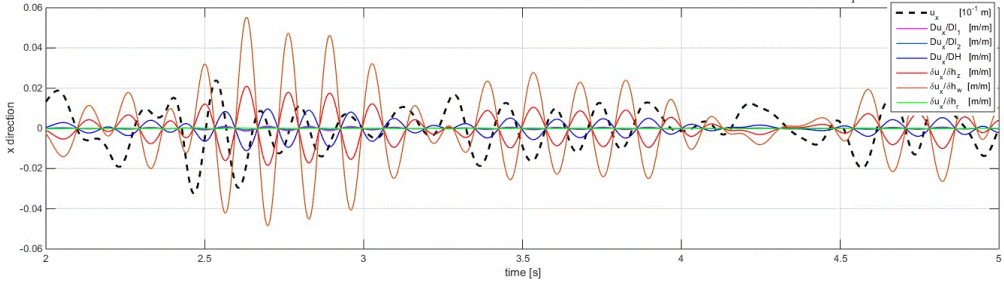


Fig. 16. Diagram of horizontal displacement $u_x(t)$ at C_4 and derivative Du_x/Dh_p

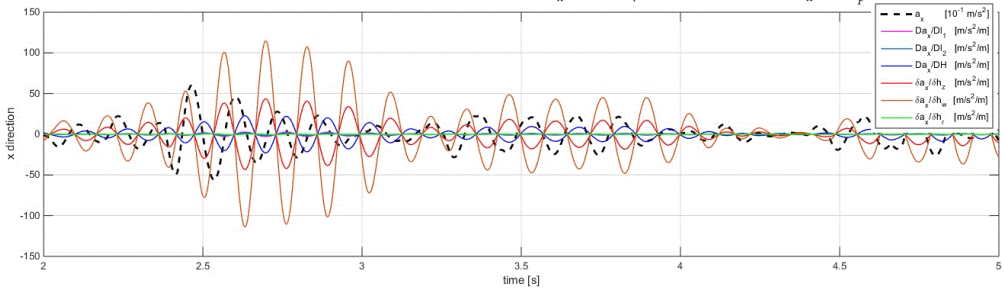


Fig. 17. Diagram of horizontal acceleration $a_x(t)$ at C_4 and derivative Da_x/Dh_p

The presented diagram Fig. 7 shows that the most intensive phase of the shock occurs up to 8 sec. and the vibrations are not steady-state. In the Fig. 14 to Fig. 17 the horizontal dynamic responses of the frame at the points C_1 and C_4 are shown in the time from 2 sec. up to 5 sec. It is obvious that the dominant response is associated with the lowest eigenfrequency f_1 of the frame.

Focusing on the most intensive phase of horizontal vibrations of the frame excited by the seismic acceleration between 2.5 sec and 3 sec. the following conclusions could be stated:

1. Amplitudes of maximum horizontal displacements and accelerations at the point C_4 (upper binder) are about twice as large as at the point C_1 (lower binder). This is related to the shape of the first eigenmode – Fig. 3.
2. In the diagrams of displacements and accelerations derivatives, three derivatives dominate: relative to h_w (cross-section height of internal pillars), h_z (cross-section height of external pillars) and H (storey height). The largest amplitude has derivative with respect to h_w . This

amplitude is about three times larger than the amplitude of the derivative with respect to h_z and about four times greater than the amplitude of the derivative with respect to H . This is reasonable because the internal pillars are connected in joints with two binders at each level and the increase of stiffness of the inner pillars more stiffens the frame for horizontal movement than increasing the stiffness of external pillars connected only to one binder at each level.

3. The largest amplitudes of derivatives occur in neighbourhood of zero displacement or acceleration, so the influence of the parameters on the responses is very strong in those points. Moreover, zeros of derivative coincide with the maxima of displacements and accelerations – the influence of the parameters on the responses should be deeply explore by higher derivatives in that points.
4. Derivative diagrams with respect to h_w and h_z are in-phase with each other – extreme amplitudes occur at the same time. The derivative with respect to H remains in the counter-phase to above ones. Thus, for example, increasing of the height of the cross-sections of pillars increases horizontal accelerations responses, the increase of the height of the storey causes the reduction of these accelerations at the same time.

5. Conclucions

Sensitivity analysis allows to get valuable information about the impact of design parameters on the response of the structure. Obtaining these derivatives could be the starting point in the optimization of the structure, optimal shaping of its geometry and optimization of cross-sections.

The presented sensitivity analysis using the DDM are efficient for models with both a few thousand degrees of freedom and a small number of design parameters. The method is simple in numerical application and gives the possibility of extensive use of parallelization of calculations.

In simpler case, direct inversion of the stiffness matrix \mathbf{K}_{ss}^{-1} and its derivatives can be avoided. The matrix \mathbf{A} (see equation (10) in [7]) must be directly expressed. It has a simple structure but in general is dependent on the parameters \mathbf{h} . In those circumstances derivatives $\mathbf{DA}/\mathcal{D}h_p$ should be explicitly specified.

References

- [1] Adhikari S., *Structural Dynamic Analysis with Generalized Damping Models. Identification*, ISTE/John Wiley & Sons, London/New York 2014.
- [2] Bathe K.-J., *Finite Element Procedures*, Prentice Hall, New Jersey 1998.
- [3] Caughey T.K., O'Kelly M.E.J., *Classical normal modes in damped linear dynamic systems*, Transactions of ASME, Journal of Applied Mechanics, 32:583–588, 1965.
- [4] CESMD, <https://strongmotioncenter.org/>, 2018.
- [5] Choi K.K., Kim N.H., *Structural Sensitivity Analysis and Optimization. Linear Systems*, Mechanical Engineering Series, Springer, New York 2005.
- [6] Choi K.K., Kim N.H., Ling F.F., *Structural Sensitivity Analysis and Optimization. Nonlinear Systems and Applications*, Mechanical Engineering Series, Springer, New York 2005.
- [7] Dąbrowska O., Ciurej H., *Sensitivity analysis of a dynamic response of a frame*, Part I: *Direct Differentiation Method*, Technical Transactions, Vol. 6/2019.
- [8] Hart G.C., Wong K., *Structural Dynamics for Structural Engineers*, John Wiley & Sons, New York 2000.
- [9] Haug E.J., Arora J.S., *Applied Optimal Design*, John Wiley & Sons, New York 1979.
- [10] Kleiber M., *Parameter Sensitivity in Nonlinear Mechanics*, Wiley, New York 1997.
- [11] Lewandowski R., *Redukcja drgań konstrukcji budowlanych*, PWN, 2014 (in Polish).
- [12] Udawadia F.E., Trifunac M.D., *Comparison of earthquake and microtremor ground motions in El Centro*, Bulletin of the Seismological Society of America, 63(4):1227–1253, 1973.



